Elias and Al-Obaydi
Journal of Engineering and Applied Science (2024) 71:28
https://doi.org/10.1186/s44147-024-00364-3

Journal of Engineering and Applied Science

RESEARCH Open Access

Effect of asymmetry pile's length on piled raft foundation system under earthquake load

Shahad Kh. Elias[1] and Moataz A. Al-Obaydi[1*]

*Correspondence: dralobaydi@uomosul.edu.iq

[1] Department of Civil Engineering, College of Engineering, University of Mosul, Mosul, Iraq

Abstract

In light of the global development of construction, particularly tall buildings and skyscrapers, researchers have spent years studying and developing types of foundations that are suitable in terms of endurance in heavily loaded and economic terms, particularly in weak soils under dynamic loading. In the event of high-rise buildings or weak soil media, the piled-raft foundation system is considered an efficient system that fits the design criteria. Several factors influence the performance of the piled-raft foundation system, among pile length, which was taken into account in the numerical study using the Plaxis 3D program. Four pile length scenarios are explored using 28 piles in a pattern 4 × 7 group with a rectangular raft of 10 × 20 and 1.5 m thickness. The central piles 3 × 2 are all the same length of 12 m or 20 m, but the others vary to 10 m, 8 m, and 6 m. In addition to the El-Centro seismic loading, a uniform static load of 300 kN/m^2 was applied to the weak C- φ soil. The results reveal that the length of the asymmetric pile has a substantial effect on the behavior of the piled raft foundation. The symmetry pile's length has greater static and dynamic load sharing than the asymmetry pile's length. Static load sharing is greater than dynamic load sharing in all models, with static sharing values of 73.2% for the uniform pile's length group L12 + 12 and 68.82%, 63.33%, and 55.96% for the asymmetry groups L12 + 10, L12 + 8, and L12 + 6, respectively. With decreasing external pile length, the dynamic load sharing values under 0.1 g intensity are 72.3%, 67.4%, 60.6%, and 55.2%, respectively. When the seismic intensity increases to 0.2 g, these values decrease by around 3%, and so on for 0.3 g. Vertical settlement increases as the exterior pile length decreases and the seismic energy increases. The maximum settlement values for L12 + 12, L12 + 10, L12 + 8, and L12 + 6 at 0.3 g seismic intensity are 137.9, 158.1, 169.7, and 171 mm, respectively. The differential settlement caused by seismic load is greater in the case of the asymmetry pile length group (L12 + 10). The differential settling increases with increasing seismic intensity in all models. The maximum lateral displacement increases as seismic intensity increases, whereas the length of the pile has no impact on the lateral displacement. When compared to a 12-m pile length, a 20-m pile will have a larger load sharing and less settlement, but exhibit a similar trend. The external pile's length has a slight effect on the factor of safety where the reduction under the seismic load by about 18% for the both symmetry and asymmetry cases respectively in comparison to static case.

Keywords: Piled-raft foundation system, Seismic load, Pile's length, Horizontal seismic coefficient

Introduction

Because of the increase in population and a shortage of land in cities, the trend is to construct high-rise buildings, which must be thoroughly investigated due to the heavy loads, particularly in the presence of earthquakes. As a result, the adoption of the piled-raft foundation system is essential in decreasing settlement and improving bearing capacity [1]. The system behaves as a combined system in which the load is shared between the piles and the raft via raft bearing, pile bearing, and pile side friction, which results in the load-sharing ratio between the raft and the piles [2]. Davis and Poulos [3] conducted the first studies that proposed an approach to examine the behavior of piled raft foundation systems, and many other researchers developed the system [4, 5]. The majority of previous studies took a static load into account. Garg et al. [6] used PLAXIS 3D to determine the most optimal values of the pile length/pile diameter ratio (Lp/dp). It was found that increasing the Lp/dp ratio enhanced the total settlement of the piled raft foundation system due to an increase in the shear resistance for side friction of the piles; nevertheless, the ratio should not exceed 30 to be more economical. Cheang et al. [7] found through the finite element method that the load carried by piles changes with the number of piles and the load type applied. Depending on the piled raft mechanism, the piles can support 70–80% of the total applied load on the foundation. In the dynamic case, Bagheri et al. [8] used the ABAQUS program to investigate the effect of earthquakes on high-rise buildings. The number of stories and the length of piles analyzed were the two primary variables. The shear force was found to be greater in the 28-m pile length than in the 10-m pile length due to more contact area with the soil around the longer piles, which causes more absorption of shear stress. However, the lateral displacement in asymmetry pile lengths of 10 m and 28 m is lesser than in symmetry pile lengths of 10 m, but greater than in symmetry lengths of 28 m. The lateral displacement increases as the number of stories increases, but in the same manner as the pile's length effect does. The global study of dynamic load sharing with varied configurations of length and number of piles found that the thickness of the raft has no effect on the dynamic axial and lateral load sharing value. However, increasing the raft thickness up to 1 m reduces vertical and lateral displacement, after which the raft thickness has no effect [2]. The frequency of the superstructure has little effect on vertical and horizontal load sharing, although it begins to increase as the number of piles increases. Furthermore, there were some peaks in vertical and lateral displacement with some frequencies as a result of the dynamic site's frequency being closed with the structure's frequency. Ibrahim et al. [9] found that the length of piles had more impact on decreasing vertical and lateral displacement under dynamic loads than the diameter. The bending moment in the square raft was generally the same with varying pile lengths, while in the rectangle raft, the bending moment reduced with increased pile length, especially when the shorter dimension of the raft was subjected to seismic. The dynamic vertical load carried by piles increases as the diameter of the pile increases, but pile position also has an effect. Chang et al. [10] showed that the smaller the diameter, the less the foundation displacement, but the relative displacement between the foundation and the soil had a considerable value. The small pile's length, on the other hand, exhibited

the opposite behavior of the diameter. The dynamic load carried by opposite seismic edge piles was greater than that carried by other edge piles, central and corner piles [8, 10]. Increased pile length resulted in improved foundation performance with fewer piles under the raft [11, 12]. The shear strain in the surrounding soil mass has been formed by the laterally loaded barrette. Plaxis 3D was utilized by Akl et al. [13] to evaluate the performance of barrettes in a single raw or group action (3×4). The findings show that the barrette shape or stiffness, soil density, and lateral load levels have minor effects on the amount of the shear strain that forms in the wedge of soil around the barrette itself. However, the strain value increases as the lateral load increases.

The soil most seriously impacted by the earthquake is soft clay. Soft soil produces a stronger bending moment along the piles and raft settlement than other soil types [5]. Few studies on the asymmetrical pile length for piled raft foundation system under dynamic load were discovered in the review literature. As a result, the influence of earthquakes on the piled raft foundation system has been investigated in this work using the PLAXIS 3D finite element method for load sharing, vertical, differential, and lateral displacements.

Methods

Numerical model

The PLAXIS 3D program was used to perform three-dimensional finite element analysis based on the direct technique to simulate the system's model for soil-piles-raft interaction (SPRI). The domain of the chosen model is based on the criteria provided by Rayhani and El Naggar [14] to avoid overlapping stresses if the model is too small or wasting time if the model is too large. As illustrated in Fig. 1, the domain dimensions are $110 \times 220 \times 30$ m. The soil is represented by a 10-node tetrahedron element, the interface by a 12-node element, the raft by a 6-node plate element, and the pile by a 3-node beam element. To avoid the earthquake from being reflected on the model, the boundary requirements for the seismic case are a free field on four vertical sides and a compliant base on four horizontal base sides.

Soil strata

The soil used in this study is C-ϕ soil, which is representative of a local site's soil type, and its parameters are shown in Table 1. The soil profile representing the local site is illustrated in Fig. 2, and the groundwater level was determined as shown in the soil profile. Accordingly, it was simulated at the lower base of the model (30 m depth).

The soil behavior is represented by a hardening with a small strain stiffness model (HSS model). Some properties were proposed based on the collected data of properties of clay soil of the local area such as saturated and unsaturated unit weight, secant stiffness, and shear strength parameters, while other values of tangent stiffness, unloading/loading stiffness, power stress level, angle of dilatancy, Shear modulus (G_o and G_s) were calculated from a mathematical relationship based on the proposed properties. The shear wave velocity was estimated based on the classification of

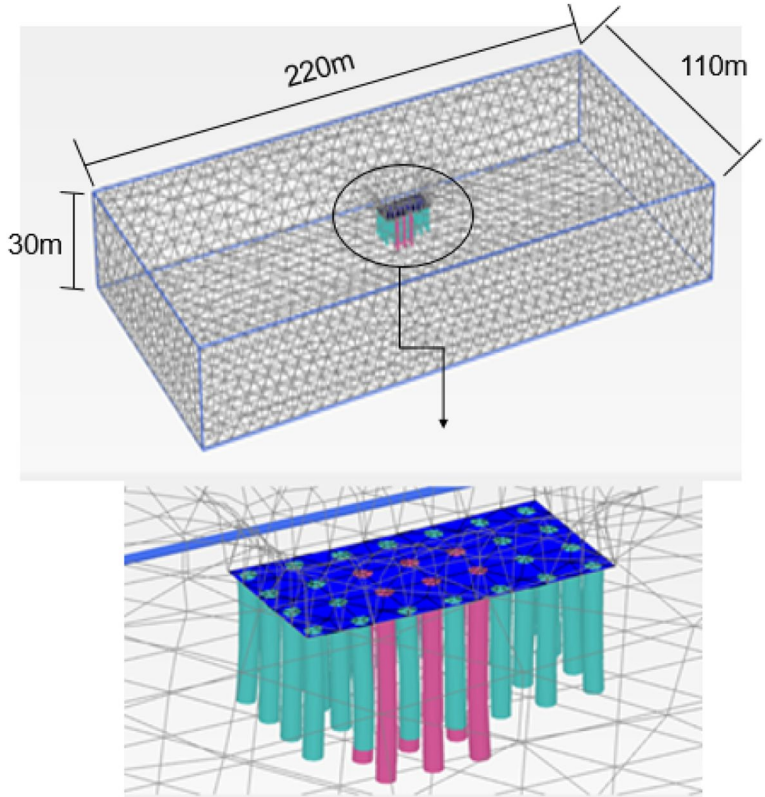

Fig. 1 Mesh and the geometry of the model

Table 1 Engineering properties of soil

Parameter	Symbol	Unit	C- φ soil
Material model	Model	---	HS
Type	---	---	Drained
Unsaturated unit weight	γ_{unsat}	kN/m^3	16
Saturated unit weight	γ_{sat}	kN/m^3	16
Secant stiffness in standard drained triaxial test	E_{50}^{ref}	kN/m^2	18000
Tangent stiffness for primary odometer loading	E_{oed}	kN/m^2	18000
Unloading/reloading stiffness	E_{ur}^{ref}	kN/m^2	54000
Power for a stress-level dependency of stiffness	m	---	1
Effective cohesion	C_{ref}	kN/m^2	10
Effective angle of internal friction	φ'	degree	22
Angle of dilatancy	ψ	degree	0
Shear strain at which $G_s = 0.722G_o$	$\gamma_{0.7}$	---	2.073E-4
Shear modulus at very small strain	$G^0{}_{ref}$	kN/m^2	78.939E3
Poisson's ratio for unloading reloading	v_{ur}'	---	0.3
Shear wave velocity	V_S	m/s	220
Damping ratio	ζ	%	3
Interface factor	R_{int}	---	0.75

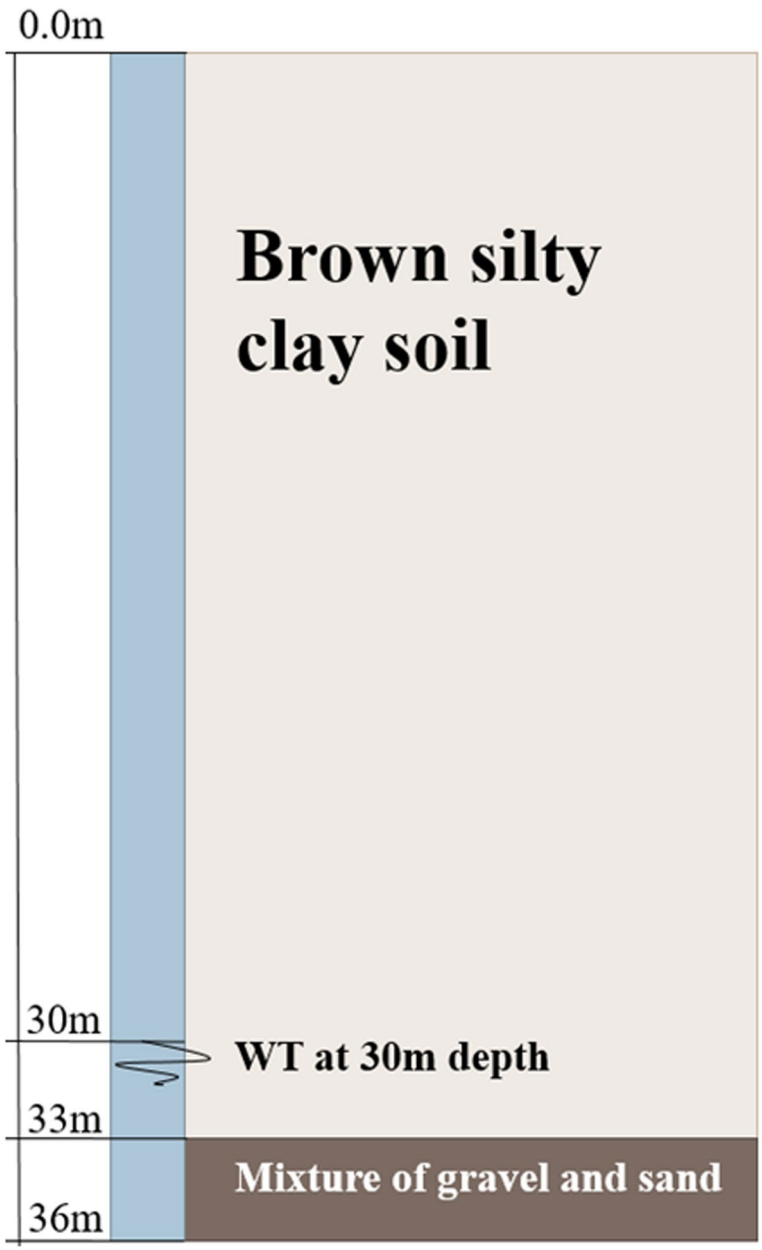

Fig. 2 Soil profile and groundwater location

Sulistiawan et al. [15]. The damping ratio is determined from the damping coefficients α and β, which are 0.5183 and 0.001302, respectively.

Structural element properties

The structural concrete elements are rafts and piles, and the building has an equivalent weight of 300 kN/m^2. The raft is composed of concrete 10 × 20 with a thickness of 1.5 m, and the piles have a number and diameter of 28 and 0.7 m, respectively, with a variable length (L). The raft and pile properties are given in Table 2, and the pile variables are listed in Table 3.

Table 2 Raft and piles properties

Parameter	Symbol	Unit	Raft	Piles	
Type	---	---	Elastic	Elastic	
Thickness of raft	D	m	1.5	---	
Unit weight	γ	kN/m^3	24	24	
Stiffness	E	kN/m^2	25.0E6	25.0E6	
Poison's ratio	V	---	0.15	0.15	
Pile's diameter	D	m	---	0.7	
Axial skin resistance	T_{max}	kN/m	---	Layer dependent	
Base resistance	F_{max}	kN	---	L = 12 m	273 kN
				L = 10 m	272.4 kN
				L = 8 m	271 kN
				L = 6 m	269.6 kN
Damping ratio	ζ	%	5	5	

Table 3 Pile's length variables

Case No	Pile length symbol	Length of central six piles (m)	Length of other piles (m)
1	L12 + 12	12	12
2	L12 + 10	12	10
3	L12 + 8	12	8
4	L12 + 6	12	6
5	L20 + 20	20	20
6	L20 + 10	20	10
7	L20 + 8	20	8
8	L20 + 6	20	6

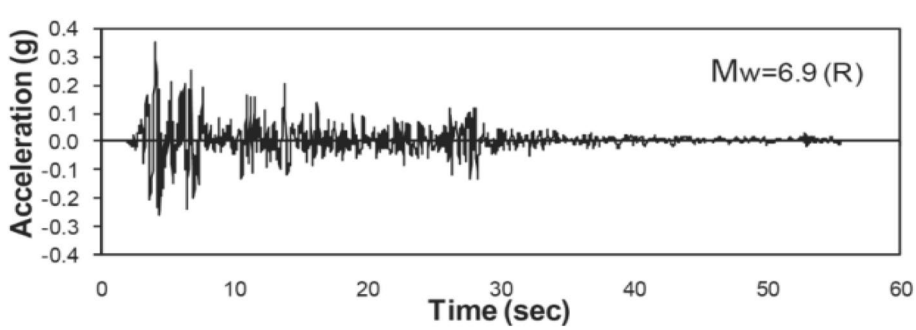

Fig. 3 Far-field acceleration record El-Centro 1940 [16]

Earthquake motion

This study utilizes the data of the El-Centro 1940 earthquake, as displayed in Fig. 3. According to Fourier spectrum curve data, the dominating frequency is 1.5–4 Hz, and the peak ground acceleration is 0.349 g. The effect of an earthquake was simulated at a depth of 30 m using a prescribed displacement surface with a horizontal *X*-axis.

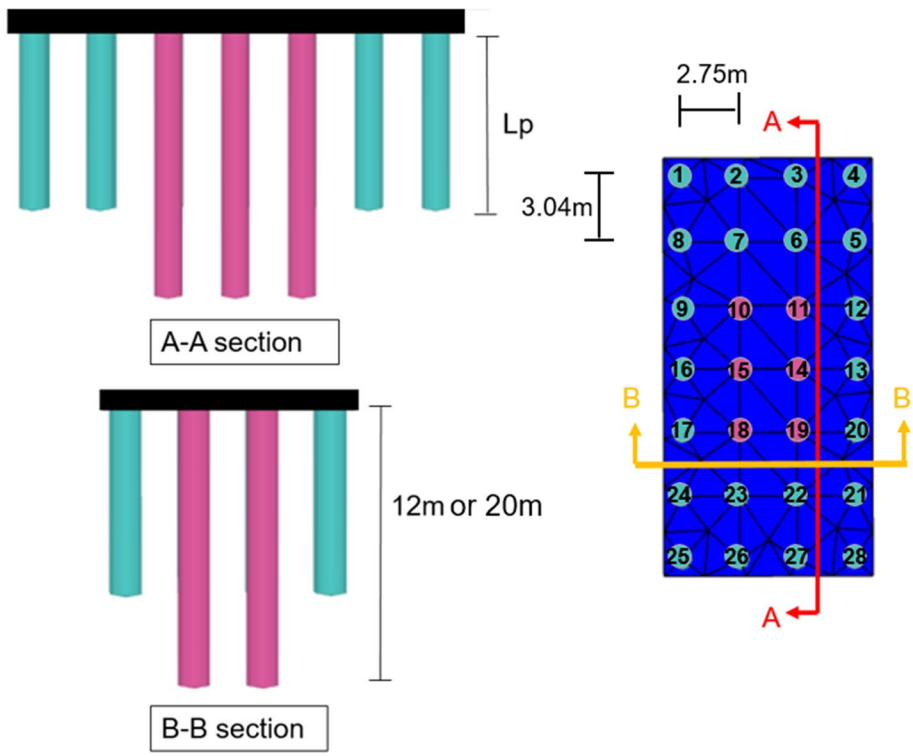

Fig. 4 Asymmetry pile's length details with bottom view of piled-raft

Parametric study

The variation of the pile's length according to four patterns, displayed in Table 3, is the most essential parameter. All piles in the first case are the same length of 12 m, in the second case the central piles are 12 m and the others are 10 m, in the third case the central piles are 12 m and the others are 8 m, and in the fourth case the central piles are 12 m and the rest are 6 m, as illustrated in Fig. 4. Seismic intensities of 0.1 g, 0.2 g, and 0.3 g were utilized. Additionally, the impact of central long piles with a 20-m length on the piled-raft foundation system was investigated in scenarios where the other exterior piles' lengths were changed to 10, 8, and 6 m.

Results and discussion

Static load sharing on asymmetry piles length

Figure 5 depicts the influence of the asymmetry pile's length on static load sharing. When the length is L12 + 12, the static load sharing by piles is 73.2%. When the length of external piles is reduced to 10 m in group L12 + 10, the static load sharing is 68.82%, 63.33% in group L12 + 8, and 55.96% in group L12 + 6. The effect of asymmetry on pile length had a significant effect on static load sharing; decreasing the external pile length caused a decrease in static load sharing by piles. The uniform pile length of L12 + 12 shows a maximum load sharing and declines gradually by decreasing pile length. This is due to a decrease in side friction as pile length decreases, resulting in a reduction in pile load sharing [11].

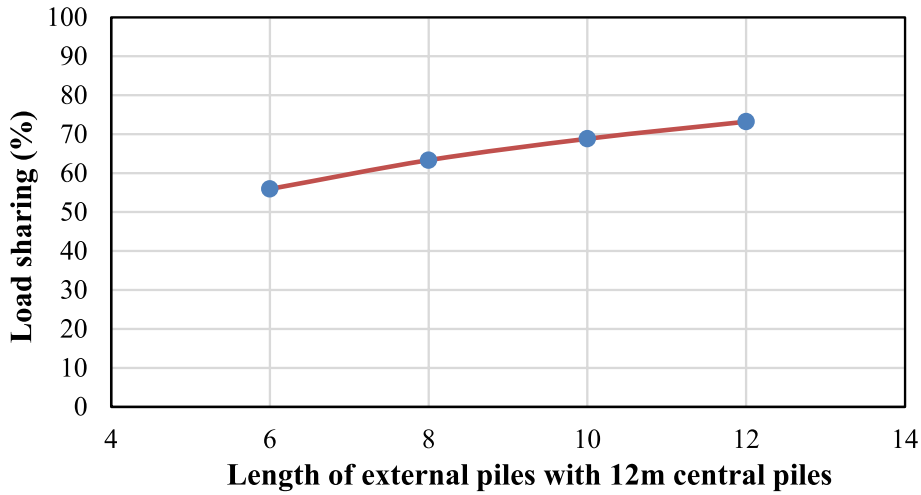

Fig. 5 Static load sharing with length of external piles

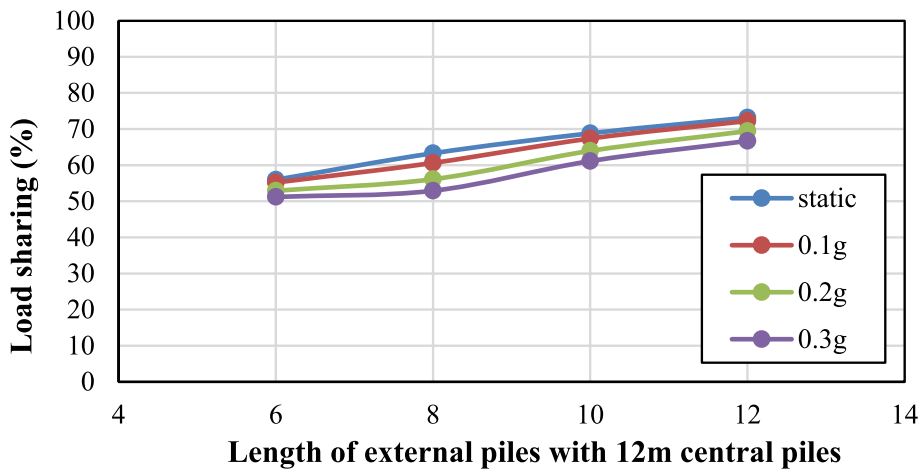

Fig. 6 Dynamic load sharing with length of external piles

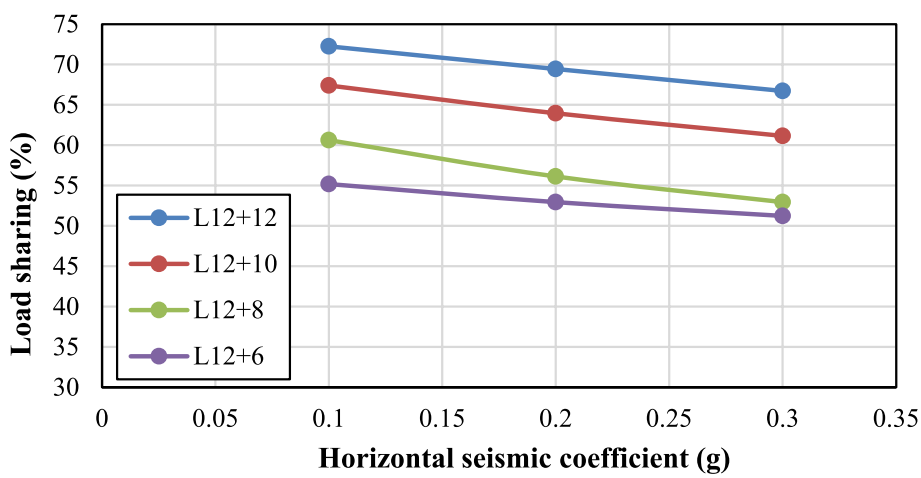

Fig. 7 Dynamic load sharing with seismic intensity

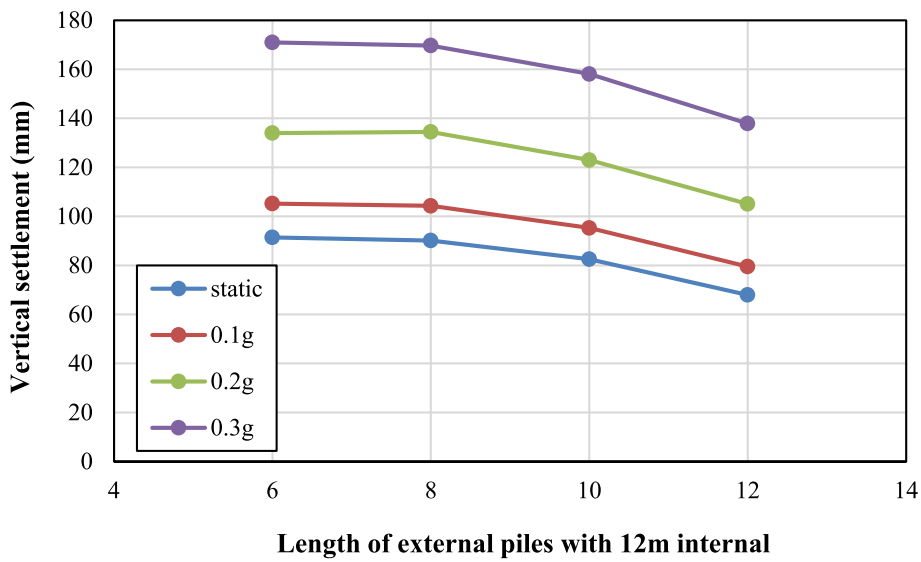

Fig. 8 Variation of the vertical settlement with the length of external piles

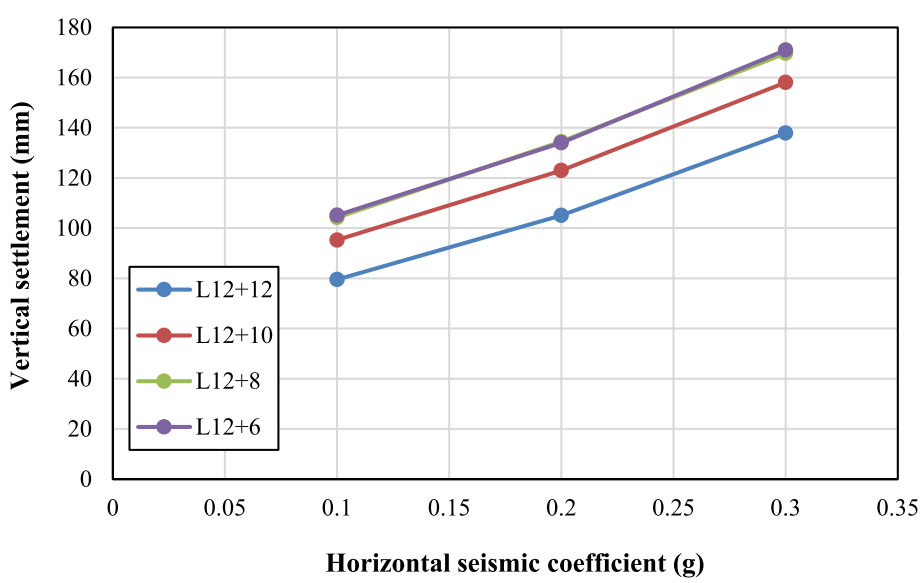

Fig. 9 Variation of the vertical settlement with seismic intensity

Dynamic load sharing with asymmetry piles length

Dynamic load sharing behaved similarly to static load sharing at 0.1 g, 0.2 g, and 0.3 g of seismic intensity, as illustrated in Figs. 6 and 7. The load sharing in the pattern of the uniform pile length (L12 + 12) is 72.255%, 69.453%, and 66.736% for seismic intensities of 0.1 g, 0.2 g, and 0.3 g, respectively. The comparable load sharing in the asymmetrical piles pattern group (L12 + 10) is 67.4%, 63.96%, and 61.163%, while it is 60.637%, 56.13%, and 52.95% in the group (L12 + 8). The pile load sharing for the asymmetric group scenario (L12 + 6) is 55.192%, 52.954%, and 51.236%. The decrease in dynamic load sharing with increasing seismic energy may be due to buckling in the piles, particularly in the long piles that cause a reduction in the pile's efficiency.

The effect of asymmetry pile's length on vertical settlement

Figures 8 and 9 depict the fluctuation of settlement with external pile length and seismic intensity. The settlement under static load for the symmetric pile group (L12 + 12) is 67.95 mm, whereas under seismic load it is 79.54 mm, 105.1 mm, and 137.9 mm for intensities of 0.1 g, 0.2 g, and 0.3 g, respectively. The static settlement of the asymmetric pile group (L12 + 10) is 82.54 mm, whereas the dynamic settlements are 95.29 mm, 123 mm, and 158.1 mm for intensities of 0.1 g, 0.2 g, and 0.3 g, respectively. Similar findings were reported by Yang et al. [17], who found that increasing seismic intensities increased vertical settlement. The static settlement values for the group (L12 + 8) are 90.14 mm, 104.3 mm, 134.5 mm, and 169.7 mm, respectively. The pile group (L12 + 6) has settlement values of 91.41 mm, 105.2 mm, 134 mm, and 171 mm. According to the results obtained by others [8, 18, 19], a decrease in pile length induced an increase in vertical settlement due to a decrease in side friction. Furthermore, increasing the seismic intensity may cause an increase in the movement and vibration of soil particles, resulting in increased loosening or densification that caused a reduction in the soil volume.

The effect of asymmetry pile's length on differential settlement

Figure 10 shows the variation of differential settlement with earthquake intensity. For the symmetric pile group (L12 + 12), the differential settlements for seismic intensity 0.1 g, 0.2 g, and 0.3 g are 7 mm, 8 mm, and 10 mm, respectively. For the asymmetric group (L12 + 10), the corresponding settlement values are 6mm, 6mm, and 10mm. The differential settlements for group (L12 + 8) are 2 mm, 4 mm, and 4.8 mm, while for group (L12 + 6) they are 3.2 mm, 4 mm, and 5 mm. The pile length has a major effect on settling, which affects the working stress, particularly in clay soil with low stiffness [20]. The working stress, bending moment, and settlement values are controlled by the length and location of the pile in the group, leading to a differential settlement.

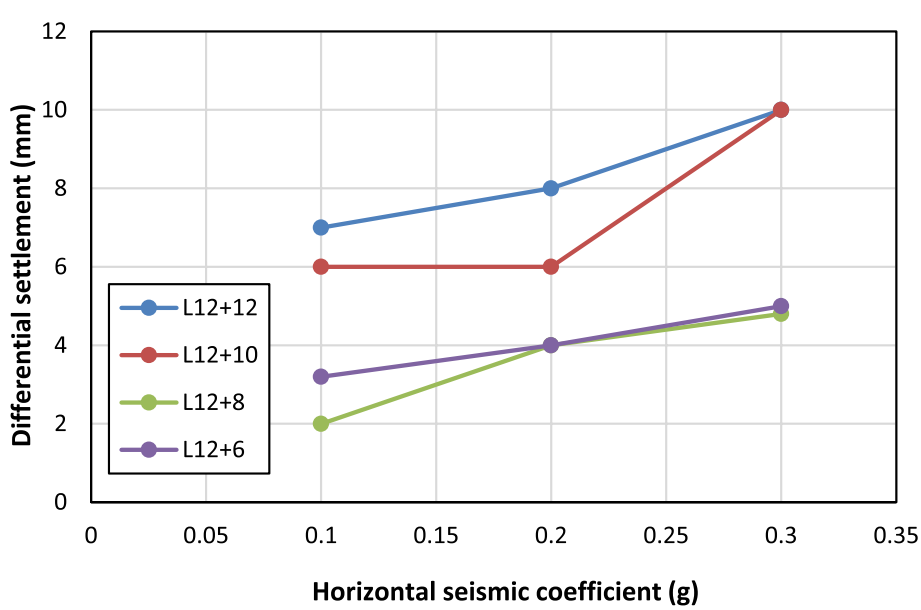

Fig. 10 Variation of the differential settlement with the seismic intensity

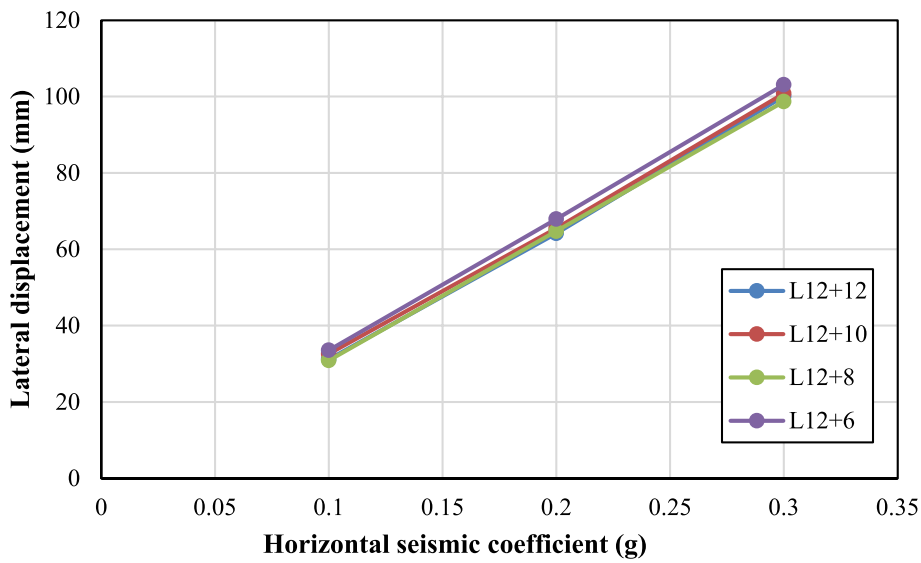

Fig. 11 Variation of lateral displacement with the seismic intensity

Table 4 Values of lateral displacement with different pile's length

Pile's length (m)	Lateral displacement (mm)		
	Horizontal seismic coefficient		
	0.1 g	0.2 g	0.3 g
L12 + 12	31.18	64.15	100.1
L12 + 10	32.61	65.5	100.8
L12 + 8	30.9	64.74	98.7
L12 + 6	33.55	67.91	103.1

The effect of asymmetry pile's length and seismic intensity on lateral displacement

Figure 11 and Table 4 illustrate the greatest lateral displacement measured at the connection point between the raft and the piles. Because of the developing lateral force, lateral displacement increases with increasing seismic intensity. Other researchers [21, 22] stated the same contribution. Meanwhile, the length of the piles has little impact on lateral displacement. This could be owing to the rigid connection between the raft and the piles and owing to the horizontal load carried by the raft exceeding the horizontal load carried by the piles [1]. It means that the raft controls the lateral displacement, while the piles have a slight effect on it regardless of pile length.

Axial force on the piles

The normal force on each pile throughout its length is shown in Fig. 12. In the static loading situation, the sum of normal forces on piles is greater than in the dynamic loading case. This could be attributed to the mechanism of the piled raft foundation system. The piles are initially designed to reach 70–80% of the ultimate load capacity before reaching full capacity, after which the raft begins to sustain its full ultimate capacity [23]. This means that the piles initially handle the majority of the load, produce buckling, and

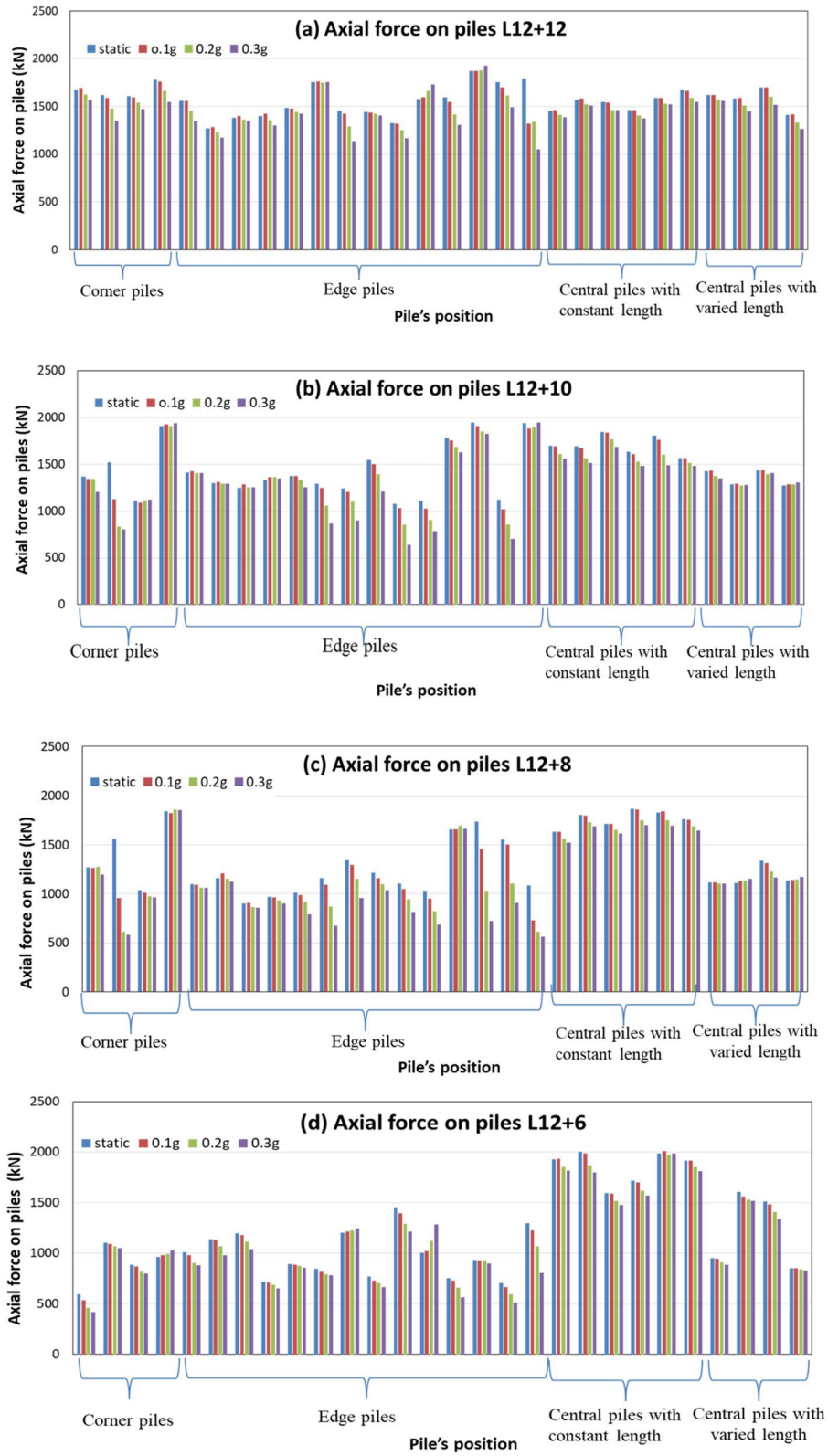

Fig. 12 The normal force on piles **a** for L12 + 12, **b** for L12 + 10, **c** for L12 + 8, and **d** for L12 + 6

reduce the pile load sharing capability under excitation. Furthermore, when the intensity of the earthquake increases, so does the deformation of the piles, and consequently, the load that is transferred to them decreases, which is dependent on the piles' efficiency. The load carried by the piles varies with their position.

Variation of vertical stress in asymmetry pile's length

The variation of the vertical stress distribution through the piled raft system in both vertical and horizontal sections is shown in Fig. 13. Stress variation cannot be clearly correlated with changes in the exterior piles' length. On the other hand, it might be

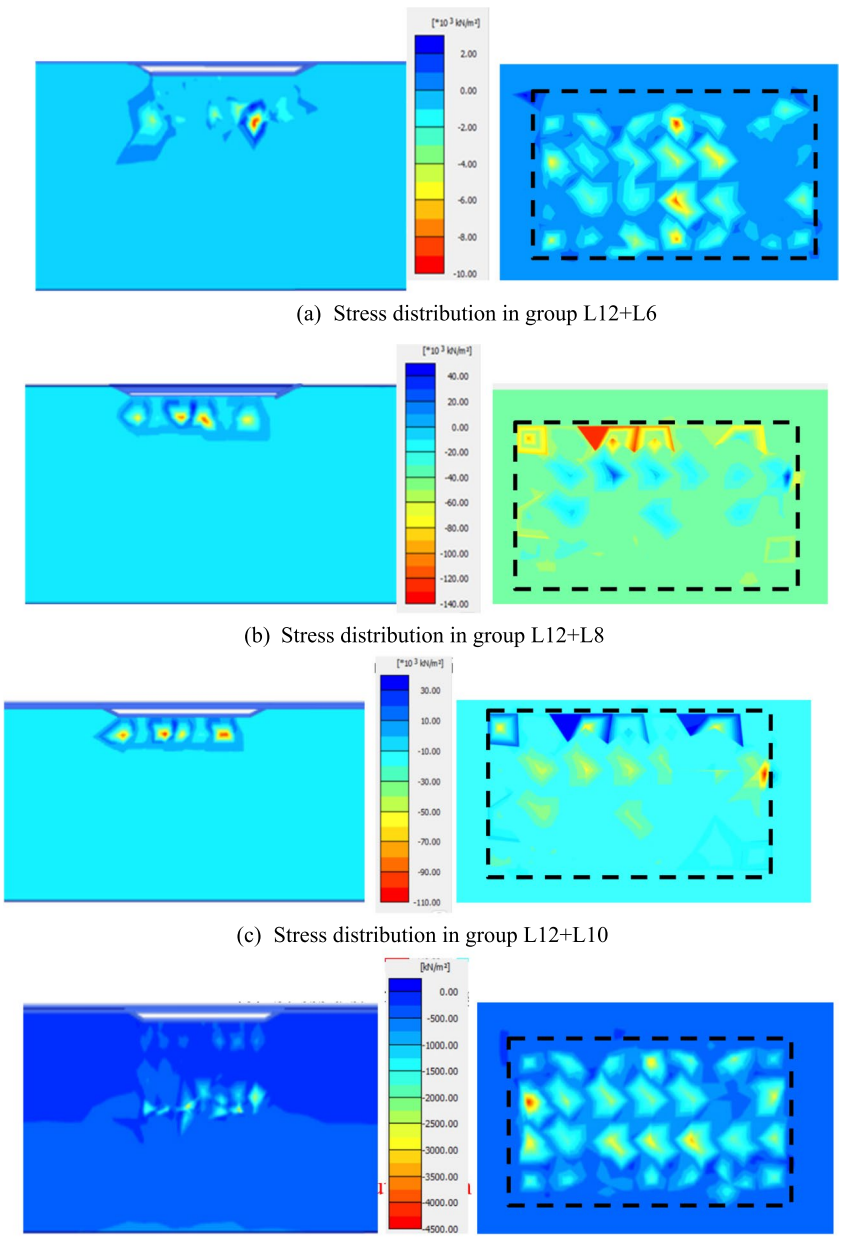

(a) Stress distribution in group L12+L6

(b) Stress distribution in group L12+L8

(c) Stress distribution in group L12+L10

(d) Stress distribution in group L12+L12

Fig. 13 Vertical stress distribution with vertical and horizontal section

said that less stress was concentrated, especially at the outside face, as a result of the exterior piles' decreasing length. The challenge of controlling the exact position of the sections taken can be attributed for these inconsistent results. Nevertheless, it can be inferred that as pile length increases, the stress beneath the raft decreases, which is related to an increase in pile load sharing.

Dynamic load sharing with asymmetry piles length using 20 m reference

The models of asymmetrical pile lengths have been regenerated in this section using a 20-m reference pile length rather than the previous section's 12 m reference. As seen in Fig. 14, the dynamic load sharing at 0.1 g, 0.2 g, and 0.3 g of seismic intensity behaved similarly to a piled raft when a 12 m reference was used. There is a comparable load sharing value of order 100% of group L20 + 20 for both the static and dynamic loads. Longer piles offer greater resistance and are able to support the load before it starts to transfer to the raft.

The load sharing values of group L20 + 10 under seismic coefficients of 0.1 g, 0.2 g, and 0.3 g are 75.04%, 72.21%, and 69.33%, respectively, whereas the static case value is 76.31%. As the exterior of piles' length is shortened, these values drop, becoming 63.465%, 63.37%, 60.89%, and 58.63% for group L20 + 6. It should be noted that the raft just acts as a load distributor when utilizing a 20-m pile length reference; it does not carry any load. However, the system is a piles cap rather than a piled raft. In the static case, the loading sharing of the 20-m-long use piles at the center is higher than that of the 12 m-long piles by 1.37, 1.11, 1.11, and 1.13 times for L20 + 20, L20 + 10, L20 + 8, and L20 + 6, respectively. Such lengthening to 20 m provides greater load sharing compared to 12 m by about 1.38, 1.11, 1.14, and 1.15 times under 0.1 g seismic intensity. The influence of the central piles' length on their load sharing increased with increasing earthquake intensity; at 0.3 g intensity, it increased by 1.50, 1.13, 1.21, and 1.14 times.

The vertical settlements while using L20 + 20 are 14.5 mm, 20.14 mm, 33 mm, and 51 mm for static, 0.1 g, 0.2 g, and 0.3 g, respectively, as illustrated in Fig. 15. The settlement value increases dramatically when the length of the central piles is shortened; for L20 + 6, the values are 78.74 mm, 90.96 mm, 116.7 mm, and 149.6 mm. Although the vertical

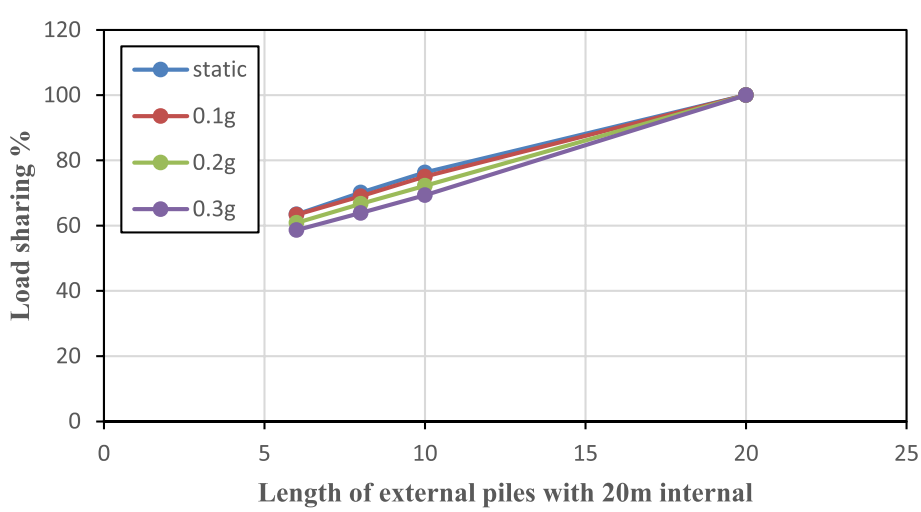

Fig. 14 The dynamic load sharing with length of external piles using 20 m reference

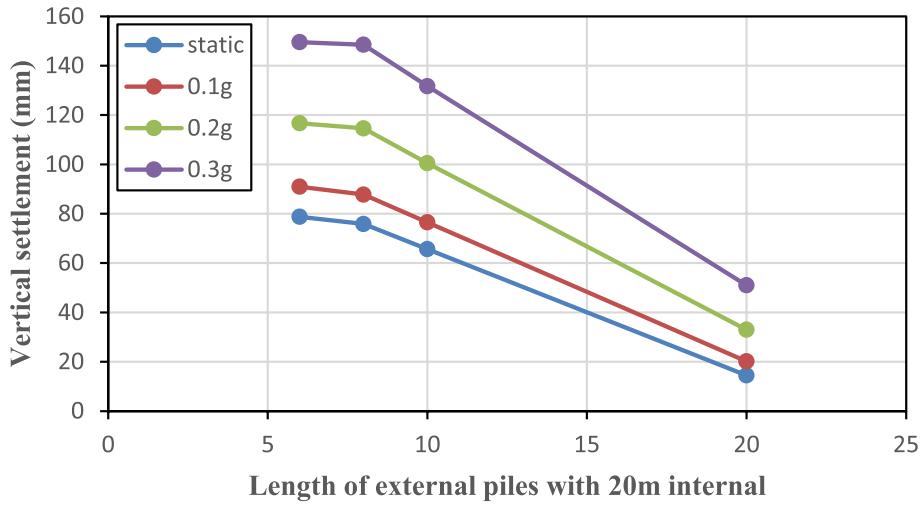

Fig. 15 Variation of the vertical settlement with the length of external piles using 20 m reference

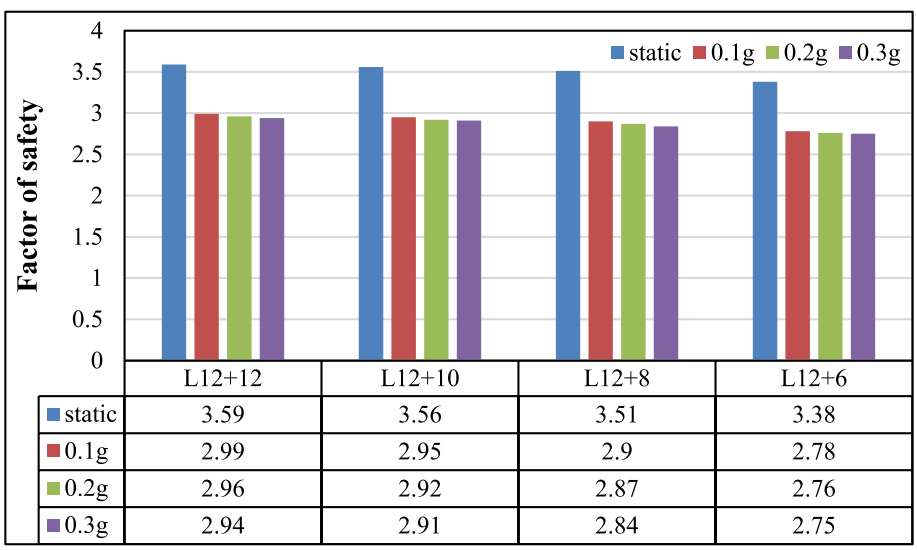

	L12+12	L12+10	L12+8	L12+6
static	3.59	3.56	3.51	3.38
0.1g	2.99	2.95	2.9	2.78
0.2g	2.96	2.92	2.87	2.76
0.3g	2.94	2.91	2.84	2.75

Fig. 16 Variation of the factor of safety with piles length and seismic intensity

settlement in 20-m piles is somewhat less than that in 12-m piles, it is nevertheless noticeable. Given that the lengthy piles provide greater side friction, this makes it reasonable.

Factor of safety of the piled-raft foundation system

As illustrated in Fig. 16, the factor of safety generally decreases in the static case as the length of the exterior piles diminishes. When the external piles' length is reduced from 12 to 6 m, the factor of safety drops from 3.59 to 3.38, which reveals the minimal impact of length on the stability under the conditions of the present study. This might not be true in other cases with different circumstances.

On the other hand, for all length variations, the safety factor decreases when an earthquake occurs. In comparison to the static case, the safety factor drops by around 18% in both cases of symmetry length (L12 + 12) and in the case of asymmetry lengths (L12 + 10, L12 + 8, and L12 + 6). The effect of the seismic intensity is insignificant in all of the cases that were examined.

Conclusions

- The vertical load sharing of both static and dynamic loadings reduces as the external pile length decreases, and the symmetry pile length L12 + 12 is optimal.
- As seismic intensity increases, vertical dynamic load sharing decreases.
- As the length of the external pile is reduced, the vertical settlement for both dynamic and static loading conditions increases.
- As seismic intensity increases, so does settling and differential settlement.
- The maximum lateral displacement is almost the same for both symmetry and asymmetry pile lengths, although it increases as seismic intensity increases.
- When comparing to a 12-m pile length, a 20-m pile has greater load sharing and less settlement.
- Under the conditions of the current study, the length of the exterior pile has little impact on the safety factor. When the pile's length drops from 12 to 6 m, it drops from 3.59 to 3.38. In comparison to the static case, the average drop in the factor of safety caused by the seismic load is around 18% in the both cases of asymmetry length.

Acknowledgements
Not applicable.

Authors' contributions
All authors have participated in the work through, prepared the data and modeling, carried out the program, analyzed the results, wrote the manuscript, and approved the final draft.

Funding
There is no funding for this manuscript.

Availability of data and materials
Not applicable in this section.

Declarations

Ethics approval and consent to participate
Not applicable in this section.

Consent for publication
Not applicable in this section.

Competing interests
The authors declare that they have no competing interests.

Received: 3 July 2023 Accepted: 8 January 2024
Published online: 31 January 2024

References

1. Al-Omari RR, Hassan AF (2013) Settlement analysis of a piled raft. Al-Rafidain Eng J 22(4):1–11
2. Karmakar S, Ranjan R, Phanikanth VS (2020) Dynamic load sharing of combined pile raft foundation (CPRF) for reinforced concrete structures. Int J Geotech Earth Eng (IJGEE) 11(1):17–44. https://doi.org/10.4018/IJGEE.2020010102

3. Davis E, Poulos H (1972) The analysis of piled raft systems. Austr Geotech J 2(1):21–27
4. Fattah MY, Al-Obaydi MA, Al-Jalabi FA (2018) Effect of number of piles on load sharing in piled raft foundation system in saturated gypseous soil. Int J Civ Eng and Techn 9(3):932–944
5. Shafiqu QM, Sa'ur RH (2018) Behavior of piled-raft foundation under earthquake loading in various types of soil. Int J Civ Eng and Techn 9(11):2770–2781
6. Garg P, Singh H, Jha J (2011) Optimization of piled-raft foundation. In: UKIERI Concrete Congress-Innovations in Concrete Construction, p 1724–1735
7. Cheang W, Phien-weij N, Almornfa K (2013) Optimization of a Piled-Raft foundation system via 3D FEM. Geotech Sustain Development-Geotec Hanoi 2013, Phung (Edt.). Construction Publisher
8. Bagheri M, Jamkhaneh ME, Samali B (2018) Effect of seismic soil–pile–structure interaction on mid-and high-rise steel buildings resting on a group of pile foundations. Int J Geomech 18(9):04018103. https://doi.org/10.1061/(ASCE)GM.1943-5622.00012222
9. Ibrahim F, El Gendy M, Salib R, El Kamash W (2003) Analysis of structures on piled raft under earthquake excitations. Sci Bull Eng Ain Shams Univ 38(3):95–114
10. Chang DW, Lee MR, Hong MY, Wang YC (2016) A simplified modeling for seismic responses of rectangular foundation on piles subjected to horizontal earthquakes. J GeoEng 11(3):109–121
11. El-Attar A (2021) Dynamic analysis of combined piled raft system (CPRS). Ain Shams Eng J 12(3):2533–2547. https://doi.org/10.1016/j.asej.2020.12.014
12. Basile F (2015) Non-linear analysis of vertically loaded piled rafts. Comp Geotech 63:73–82. https://doi.org/10.1016/j.compgeo.2014.08.011
13. Akl SAY, Ismail AN, Abdelmoghni M, Hegazy YA (2023) Numerical analysis of laterally loaded barrettes performance in cohesionless soils. J Eng App Sci 70:51. https://doi.org/10.1186/s44147-023-00219-3
14. Rayhani MH, El Naggar MH (2008) Numerical modeling of seismic response of rigid foundation on soft soil. Int J Geomech 8(6):336–346. https://doi.org/10.1061/(ASCE)1532-3641(2008)8:6(336)
15. Sulistiawan H, Supriyadi S, Yulianti I (2018) Shear wave velocity profiling analysis for site classification using microtremor single station method. In: AIP conference Proceedings 2014(1). AIP Publishing, Surakarta. https://doi.org/10.1063/1.5054407
16. Tabatabaiefar S, Fatahi B, Samali B (2014) Numerical and experimental investigations on seismic response of building frames under influence of soil-structure interaction. Adv Struct Eng 17(1):109–130. https://doi.org/10.1260/1369-4332.17.1.109
17. Yang Y, Gong W, Cheng YP, Dai G, Zou Y, Liang F (2021) Effect of soil-pile-structure interaction on seismic behaviour of nuclear power station via shaking table tests. In Structures 33:2990–3001. https://doi.org/10.1016/j.istruc.2021.06.051
18. Beygi M, Keshavarz A, Abbaspour M, Vali R (2020) 3D numerical study of the piled raft behaviour due to groundwater level changes in the frictional soil. Int J Geotech Eng 14(6):665–672. https://doi.org/10.1080/19386362.2019.1677326
19. Rasheed AH, Qasim OA, Al-Quraishy QA (2020) Behavior of pile rafts with raft size, number of piles and different pile length. AIP Conf Proc 2213(1):020196. https://doi.org/10.1063/5.0000211. AIP Publishing LLC
20. Akl AY, Mansour MH, Moustafa HK (2014) Effect of changing configurations and lengths of piles on piled raft foundation behaviour. Civ Eng Urban Plann: An Int J 1(1):49–65
21. Kumar A, Choudhury D, Katzenbach R (2016) Effect of earthquake on combined pile–raft foundation. Int J Geomech 16(5):04016013. https://doi.org/10.1061/(ASCE)GM.1943-5622.0000637
22. Halder P, Manna B (2019) Seismic analysis of piled raft foundation—pseudostatic approach. In: Earth Geotech Eng Prot Develop of Envir Constr. CRC Press, Rome, p 2771–2778
23. Das BM, Sivakugan N (2018) Principles of foundation engineering. Cengage learning

Publisher's Note